Functional and Molecular Reorganization of the Nucleolar Apparatus in Maturing Mouse Oocytes

Olga V. Zatsepina,*,† **Christine Bouniol-Baly,**† **Claudine Amirand,**‡
and Pascale Debey†

**A. N. Belozersky Institute of Physical and Chemical Biology, Moscow University, Moscow
119899, Russia;* †*Institut National de la Recherche Agronomique 806/EA 2703, IFR 63,
Muséum National d'Histoire Naturelle, Institut de Biologie Physico-Chimique, 13 Rue Pierre et
Marie Curie, 75005 Paris, France; and* ‡*Centre National de la Recherche Scientifique ESA 7033,
Université Pierre et Marie Curie, 75005 Paris, France*

In mammalian preovulatory oocytes, rRNA synthesis is down-regulated until egg fertilization and zygotic genome reactivation, but the underlying regulatory mechanisms of this phenomenon are poorly characterized. We examined the molecular organization of the rRNA synthesis and processing machineries in fully grown mouse oocytes in relation to ongoing rDNA transcription and oocyte progression throughout meiosis. We show that, at the germinal vesicle stage, the two RNA polymerase I (RNA pol I) subunits, RPA116 and PAF53/RPA53, and the nucleolar upstream binding factor (UBF) remain present irrespective of ongoing rDNA transcription and colocalize in stoichiometric amounts within discrete foci at the periphery of the nucleolus-like bodies. These foci are spatially associated with the early pre-rRNA processing protein fibrillarin and in part with the pre-ribosome assembly factor B23/nucleophosmin. After germinal vesicle breakdown, the RNA pol I complex disassembles in a step-wise manner from chromosomes, while UBF remains associated with chromosomes until late prometaphase I. Dislodging of UBF, but not of RNA pol I, is impaired by the phosphatase inhibitor okadaic acid, thus strengthening the idea of a relationship between UBF dynamics and protein phosphorylation. Since neither RNA pol I, UBF, fibrillarin, nor B23 is detected at metaphase II, i.e., the normal stage of fertilization, we conclude that these nucleolar proteins are not transported to fertilized eggs by maternal chromosomes. Together, these data demonstrate an essential difference in the dynamics of the major nucleolar proteins during mitosis and meiosis.   © 2000 Academic Press

Key Words: nucleolus; mouse oocytes; meiotic maturation; gene expression; phosphorylation.

INTRODUCTION

In all species so far examined, oocyte maturation is accompanied by profound transformations of their metabolism. In mammals, RNA synthesis occurs at a low rate in oocytes of primordial follicles but increases during the oocyte growth and reaches a peak at the beginning of antrum formation (Bloom and Mukherjee, 1972; Moore *et al.,* 1974; Wassarman and Letourneau, 1976). Preantral oocytes accumulate a vast amount of messenger, ribosomal, and transfer RNAs; ribosomes; and proteins that will be utilized at early stages of embryonic development (Kaplan *et al.,* 1982; Taylor and Piko, 1982). Analysis of the RNA content indicated that about 65% of it is ribosomal RNA (Wassarman, 1988). In fully grown mouse oocytes at the germinal vesicle (GV) stage, the synthesis of mRNAs and

rRNAs declines (Moore *et al.,* 1974; Kaplan *et al.,* 1982), yet those which are characterized by a relatively dispersed chromatin configuration ("nonsurrounded nucleolar" oocytes, NSN oocytes; Debey *et al.,* 1993) remain transcriptionally active and synthesize all classes of RNA (Bouniol-Baly *et al.,* 1999). In contrast, no BrUTP incorporation is observed in the fully grown GV oocytes exhibiting a condensed perinucleolar chromatin ring ("surrounded nucleolar" oocytes, SN oocytes; Debey *et al.,* 1993; Bouniol-Baly *et al.,* 1999), which apparently represent the most advanced stage of preovulatory GV oocytes (Mattson and Albertini, 1990; Zuccotti *et al.,* 1995, 1998). Also no RNA synthesis was registered after the germinal vesicle breakdown (GVBD) or during the two subsequent meiotic divisions (Bloom and Mukherjee, 1972; Moore *et al.,* 1974; Rodman and Bachvarova, 1976; Wassarman and Letourneau, 1976).

The growth of mouse oocytes is accompanied by drastic morphological changes of the nucleolar apparatus. The vacuolated and fibrillogranular nucleolus characteristic of the actively transcribing primary oocytes is gradually transformed into a nearly homogeneous and compact mass in fully grown oocytes (Chouinard, 1971; Mirre and Stahl, 1981; Tesarik *et al.,* 1984; Antoine *et al.,* 1988, 1989; Crozet, 1989). This "mass" is referred to as the nucleolus-like body (NLB; Tesarik *et al.,* 1984; Kopecny *et al.,* 1995). The NLBs lack DNA but are mainly composed of ribonucleoproteins (RNPs) and silver-negative proteins of uncertain origin (Antoine *et al.,* 1988, 1989), whereas their periphery is associated with the Ag-NOR (nucleolus organizing region) binding proteins (Takeuchi, 1984; Antoine *et al.,* 1988) that are known to be physiological markers of ongoing rDNA transcription in somatic cell nucleoli (Hubbel, 1985). NLBs were also shown to contain U3 SnRNPs (Prather *et al.,* 1990) and nonnucleolar spliceosomal factors (Kopecny *et al.,* 1996). However, the precise composition of NLBs and their role in ribosome biogenesis still remain to be established. Also, very little is known about the fate of NLB material after nucleolar disassembly at the GVBD stage.

In somatic cells, the accurate and efficient transcription of the ribosomal genes encoding 18S, 5.8S, and 28S rRNA (rDNA) requires a multidomain transcription machinery, which is composed of a number of RNA pol I subunits, a few pol I-associated factors (PAFs), and at least two specific transcription initiation factors. One of them is a multiprotein complex SL1, (TIF-IB in mice; Schnapp *et al.,* 1994), that consists of the TATA box-binding protein (TBP) and three TBP-associated factors (Rudloff *et al.,* 1994; Heix *et al.,* 1998). The other one is the upstream binding factor, UBF (Jantzen *et al.,* 1990; Voit *et al.,* 1992). UBF is the most abundant and therefore the most well-characterized nucleolar transcription activator. It may help to organize the promoter region of the rDNA in such a way that RNA pol I (together with other factors) can form a stable preinitiation complex (Hernandez, 1993; Bazett-Jones *et al.,* 1994; Reeder *et al.,* 1995). Surprisingly, in all somatic cells so far examined, the major compounds of the RNA pol I transcription machinery remain bound to rDNAs, irrespective of their transcription status. Thus, RNA pol I, UBF, and the TATA-binding protein/SL1 remain bound to the ribosomal genes (chromosomal NORs) in serum-deprived cells, where rRNA synthesis is partially suppressed, and also during mitosis, when no rDNA transcription occurs (Zatsepina *et al.,* 1993; Jordan *et al.,* 1996; Roussel *et al.,* 1996, Seither *et al.,* 1997). These facts indicate that physical dislodging of RNA pol I transcription complex from the ribosomal genes is unlikely to control the rRNA synthesis in somatic cells (Weisenberger and Scheer, 1995). Recent findings afford strong evidence that the cell-cycle and growth-dependent controls of rRNA synthesis are primarily mediated by phosphorylation of the basal transcription factors, which either negatively or positively modulate RNA pol I transcription during somatic cell cycle (Voit *et al.,* 1992; Kihm *et al.,*

1998; Tuan *et al.,* 1999). The specific cellular kinases involved in this regulation and their target residues in the UBF and SL1 factors have been identified (Heix *et al.,* 1998; Voit *et al.,* 1999).

In contrast to mitotic cycles, essentially nothing is known about the mechanisms which control the rDNA switch-off during meiosis. Moreover, the molecular organization of the RNA pol I transcription machinery in maturing mammalian oocytes has not been examined. Also, posttranscriptional events that occur during oocyte maturation are poorly documented, and the question of whether the key rRNA processing proteins, such as an early pre-rRNA processing protein, fibrillarin (Lazdins *et al.,* 1997), and a pre-ribosome assembly factor, B23/nucleophosmin (reviewed by Shaw and Jordan, 1995; Zatsepina *et al.,* 1997), follow the same pathways at meiosis and mitosis still remains to be examined.

Using different experimental approaches, such as high-resolution immunofluorescence microscopy with antibodies against two RNA pol I subunits and UBF, detection of run-on rDNA transcription by incorporation of BrUTP, computer analysis of the spatial distribution of fluorescent probes, and Western blots, we have studied the dynamics of the rDNA transcription complex in maturing mouse oocytes. We show that the rDNA transcription complex remains spatially associated with NLBs in mouse GV oocytes, irrespective of the ribosomal gene activity, but is dislodged from meiotic chromosomes after GVBD. We present evidence that UBF detaches from the prometaphase I chromosomes later than RNA pol I and that this event is dependent on the protein phosphorylation status. At MII stage, UBF and RPA116 appear largely degraded. Neither rDNA transcription (RNA pol I, UBF) nor rRNA processing (fibrillarin, B23) proteins are transported to the fertilized zygote by maternal chromosomes. This implies that reinitiation of rRNA synthesis in early embryos requires *de novo* synthesis and assembly of factors of the RNA pol I preinitiation complex and their interaction with the rDNA template.

MATERIALS AND METHODS

Recovery, Selection, and in Vitro Culture of Oocytes

Ovaries were isolated from 4- to 6-week-old C57 × CBA female mice. The fully grown GV oocytes (about 70 μm in diameter) were collected by random puncturing of antral follicles, freed from follicular cells by a gentle pipetting, and kept in M2 medium (Fulton and Whittingham, 1978) at 37°C until use. To prevent spontaneous maturation of oocytes, 100 μg/ml dibutiryl cAMP (dbcAMP; Sigma, St. Louis, MO) was added to M2 medium. Alternatively, oocytes cultured without dbcAMP passed GVBD within 1 to 3 h postisolation and progressed to prometaphase I (6–7 h), metaphase I (MI; 7–9.5 h), and MII (11–13 h) stages, when they became naturally arrested (Wassarman, 1988; Debey *et al.,* 1993). To obtain the *in vivo* matured MII oocytes, 4- to 6-week-old females were superovulated with ip injection of 5 IU of pregnant

mare serum gonadotropin (Intervet, Angers, France) followed 48 h later with 5 IU of human chorionic gonadotropin (hCG; Intervet, Chorulon, France) and sacrificed 14 h after the hCG injection. MII oocytes were directly collected from ampullae, released from cumulus cells with 1 mg/ml hyaluronidase for 2 min, and used immediately.

Assessment of rRNA synthesis was monitored following Bouniol-Baly *et al.* (1997). Isolated GV oocytes were incubated with 100 μg/ml dbcAMP and 10 μg/ml α-amanitin (Sigma) for 30 min prior to microinjection. Oocytes were microinjected into the cytoplasm with 1 $\pm$ 0.5 pl of a solution containing 100 mM BrUTP (Sigma), 50 μg/ml α-amanitin, 140 mM KCl, 2 mM Pipes, pH 7.4; recovered in M2 containing dbcAMP and α-amanitin for 10–30 min; rinsed; and fixed for the immunolabeling procedures. Such conditions of α-amanitin treatment were previously shown not to affect the nucleolar morphology and activity (Masson *et al.,* 1996, and unpublished observations).

Drug Treatments

Isolated GV oocytes were cultured in M2 medium containing either 1 μM okadaic acid (OA; Sigma), a potent type-1 and type-2A phosphatase (PP2A) inhibitor (Gavin *et al.,* 1992; Labhart, 1994), or 2.5 mM 6-dimethylaminopurine (6-DMAP; Sigma), a general kinase inhibitor (Szöllösi *et al.,* 1991; Labhart, 1994), up to 9 h after collection. Since 6-DMAP is known to prevent oocytes from undergoing GVBD (Szöllösi *et al.,* 1991), it was added to M2 medium shortly after the nuclear dissolution (early GVBD), which was monitored under a dissection microscope.

Antibodies and Immunolabeling

Isolated oocytes were fixed either with 4% paraformaldehyde (PFA) for 20 min or with 80% methanol for 40 min, permeabilized with 0.2% Triton X-100 in PBS for 15 min, blocked in 2% BSA in PBS, and processed for *in toto* single or double immunolabelings (see below). All steps were performed at room temperature. Alternatively, oocytes were fixed with 4% PFA for 40 min and embedded in 20% gelatin following Vautier *et al.* (1994). Serial cryosections (3–5 μm) from individual oocytes were made using 2800 Frigocut (Reichert-Jung, Austria) at $-28°$C, collected on Superfrost slides (O. Kindler GmbH & Co, Freiburg, Germany), and stored at $-70°$C until use.

Immunostaining reactions were performed using appropriate combinations of the following primary antibodies: human anti-UBF serum (Zatsepina *et al.,* 1993; dilution 1:100 in PBS supplemented with 2% BSA); rabbit polyclonal serum or affinity-purified antibody against an RNA pol I-associated factor, PAF53/RPA53 (Seither *et al.,* 1997; dilutions 1:25 and 1:50, respectively); mouse polyclonal serum against a 116-kDa subunit of RNA pol I, RPA116 (dilution 1:70; anti-RPA116 and anti-PAF53/RPA53 were gifts from Dr. I. Grummt, German Cancer Research Center, Heidelberg, Germany); human autoimmune serum against fibrillarin (Magoulas *et al.,* 1998; dilution 1:100); mouse mAb to fibrillarin (a gift from Dr. R. Ochs, W. M. Kerk Autoimmune Disease Center, La Jolla, CA; Ochs and Press, 1992); mouse mAb to B23/nucleophosmin (Zatsepina *et al.,* 1997; a gift from Dr. P. K. Chan, Baylor College of Medicine, Houston, TX; dilution 1:50); mouse mAb against BrdU that also recognizes BrU (Boehringer, Mannheim, Germany; dilution 1:50).

Whole oocytes or their sections were incubated with the primary antibodies for 1 h at room temperature or overnight at 4°C, washed

in 2% BSA for 1 h, and incubated with the secondary antibodies for 40 min. As secondary antibodies, anti-human FITC-conjugated IgGs (Sigma; dilution 1:50), anti-human DTAF-conjugated IgGs (Jackson Immunoresearch Laboratories, Inc., West Grove, PA; dilution 1:50), anti-mouse Cy3-conjugated IgGs (Dianova, Hamburg, Germany; dilution 1:300), anti-mouse FITC-conjugated IgGs (Jackson Immunoresearch Laboratories; dilution 1:50), and anti-rabbit Texas red-conjugated IgGs (Sigma; dilution 1:100) were used. Specimens were stained with 1 μg/ml Hoechst 33242 for 30 min and, after thorough washing with PBS, were mounted in Citifluor (Citifluor Products, Canterbury, UK). For each data point, 12 to 42 oocytes were examined.

For immunofluorescence controls, PBS was used instead of the primary antibodies. The specificity of BrUTP incorporation into the newly synthesized rRNA was tested by oocyte incubation with 0.2–0.5 μg/ml actinomycin D (Sigma) for 1–3 h, which completely inhibited BrUTP incorporation. Noteworthy, patterns of oocyte immunolabeling were basically the same in PFA- and methanol-fixed specimens.

Fluorescence Microscopy and Image Analysis

Conventional fluorescence microscopy was performed on a Axiovert inverted microscope (Carl Zeiss, Oberkochen, Germany) using a filter wheel for the excitation light, a triple-band dichroic mirror and filter set for emitted light, and a 100$\times$ Plan Neofluar objective (NA 1.3). Serial optical sections were captured by a cooled CCD camera (Photometrics, Tucson, AZ; type KAF 1400, 12 bits of dynamic range) and processed through the IPLab Spectrum software (Vysis, France). With this setup, images taken at two different wavelengths differed at most by a translation of one pixel. In addition, we checked that there was absolutely no overlap between rhodamine and fluorescein signals using this combination of filters. Confocal microscopy was performed on an upright Nikon microscope equipped with the Bio-Rad LaserSharp MRC-1024 confocal laser scanning software. The objective was a Nikon Fluor oil immersion 100$\times$ (NA 1.3) and the pinhole was set at its optimum size (3.4 mm). The 488- and 568-nm wavelengths of the laser were used for fluorescein and Texas red excitation, respectively.

The spatial distribution of two selected probes labeled with fluorochromes was analyzed using a software developed in our laboratory (SPIMAC, "Spectral Imaging on Macintosh"; Amirand *et al.,* 1998). Briefly, the software provides a 2D histogram in which x and y coordinates represent the normalized gray levels of the same pixel in the two images. Different subpopulations of pixels can then be identified as different regions of the 2D histogram. The linear correlation coefficient (r) between x and y values for a selected pixel population can be calculated.

Western Blots

One hundred to 150 oocytes at the GV stage or 150 to 200 oocytes at the MII stage were added to 10 μl of Laemmli buffer (Laemmli, 1970), denatured by heating to 95°C for 7 min, and subjected to 10% SDS–PAGE. Fractionated proteins were transferred onto 0.22-μm nitrocellulose (Bio-Rad, Hercules, CA) following a standard procedure. The membrane was blocked with 5% skim milk in PBS containing 0.1% Tween 20 for 1 h and incubated with the anti-RPA116 polyclonal antibody (dilution 1:4000 in PBS containing 3% BSA) or the anti-UBF serum (dilution 1:5000) for 1 h at room temperature, which was followed by horseradish peroxidase-conjugated secondary antibodies (Sigma; dilution
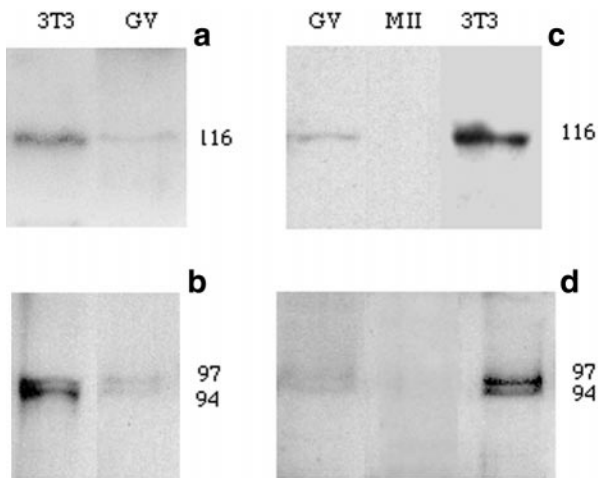
FIG. 1. Anti-RPA116 mouse polyclonal antibody (a, c) and anti-UBF serum (b, d) recognize the relevant epitopes on Western blots of protein extracts prepared from cultured NIH3T3 cells (3T3) and mouse GV oocytes (GV), but not from MII (MII) oocytes. Extracts from 1.2×10^4 NIH3T3 cells, 100 (a and b) or 150 (c and d) GV and 150 (c) or 200 (d) MII oocytes were separated by 10% SDS–PAGE, transferred to nitrocellulose filters, and probed with anti-RPA116 (a, c; dilution 1:4000) or anti-UBF (b, d; dilution 1:5000) antibodies.

1:100,000) for 40 min. The nitrocellulose was developed using the Pierce SuperSignal ULTRA chemiluminescence detection system (Interchim, Montluçon, France). For controls, total NIH3T3 cell extracts were prepared essentially following the same protocols. Each experiment was repeated five times with similar results.

RESULTS

To study the dynamics of the RNA pol I transcription complex in mouse oocytes, we selected antibodies which are known to recognize antigens in mouse NIH3T3 fibroblasts on Western blots and by immunofluorescence (for UBF, see Zatsepina *et al.,* 1993; for RPA116 and PAF53/RPA53, Seither *et al.,* 1997; for fibrillarin and B23, Magoulas *et al.,* 1998). Western blot analysis of total oocyte extracts further demonstrated that the anti-UBF serum and anti-RPA116 antibody specifically recognize the epitopes in mouse GV oocytes as well (Fig. 1). Like in total NIH3T3 cell extracts, RPA116 was recovered as a single band with M_r 116 kDa (Figs. 1a and 1c) and UBF as a double band with M_r 94 and 97 kDa (Figs. 1b and 1d). Antigen-binding capacities of the PAF53/RPA53 antibody were insufficient to recognize the protein on Western blots using a reasonable number of oocytes (not shown). However, like others, the anti-PAF53/RPA53 antibody was sensitive enough for immunolabeling of oocytes *in situ* (see below).

The rDNA Transcription and Early Pre-rRNA Processing Machineries Are Associated with the Periphery of NLBs in Transcriptionally Competent GV Oocytes

In the first series of experiments, we analyzed the RNA pol I transcription complex in GV oocytes which were attributed to the NSN group because of their chromatin configuration (Debey *et al.,* 1993). NSN oocytes were fixed *in toto* and probed for UBF and for either of the RNA pol I subunits. A typical UBF and RPA116 labeling pattern is shown in Fig. 2a for different optical sections of the same oocyte. One can see that both signals are associated solely with the NLB surface and distributed between the same discrete and numerous beads ($n = 20$ to 40 per oocyte) of 0.2–1 μm in size (Figs. 2a and 2c). In some cases, the smallest beads are separated by strikingly regular intervals of about 1 μm length (Fig. 2c), thus giving an appearance of single ribosomal rDNA repeats interrupted by intergenic spacers similar to that in 5,6-dichloro-1-α-D-ribofuranosylbenzimidazole-treated somatic nucleoli (Le Panse *et al.,* 1999). Similar results were obtained when oocytes were processed for double immunolabeling for UBF and PAF53/RPA53 (not shown).

In keeping with the data that, in somatic cells, PAF53/RPA53 might be more loosely associated with—and more easily dislodged from—RNA pol I complex than the genuine RNA pol I subunit (RPA116; Hanada *et al.,* 1996), NSN oocytes were further processed for double immunolabeling with anti-RPA116 and anti-PAF53/RPA53 antibodies. A typical labeling pattern is shown in Fig. 2b. As one can see, three of the main compounds of RNA pol I complex are present and entirely coincident in transcriptionally competent NSN-type GV oocytes, as they are in active mouse 3T3 fibroblasts (Seither *et al.,* 1997).

To examine whether local concentrations of UBF and RNA pol I were correlated in each point, we quantitatively analyzed couples of images from double immunofluorescence labeling using the SPIMAC software (Amirand *et al.,* 1998). The 2D histogram obtained from one of the optical sections of Fig. 2a is displayed in Fig. 3a. It shows that intensities of UBF and RPA116 immunolabeling in each pixel of the images are linearly correlated ($r = 0.95$). Similar results were obtained for RPA116 and PAF53/RPA53 (not shown). These data clearly demonstrate that UBF, PAF53/RPA53, and RPA 116 are not only present in the same foci, but colocalize there in a constant stoichiometry.

As the RNA pol I transcriptional machinery is associated with the NLB surface (Fig. 2), and rRNA synthesis occurs at the NLB surface in transcriptionally competent NSN oocytes (Bouniol-Baly *et al.,* 1999), we particularly focused on the spatial relationship between RNA pol I, UBF, and nascent rRNA transcripts. For this, NSN oocytes were microinjected with BrUTP in the presence of α-amanitin at a concentration known to inhibit RNA pol II only, double immunolabeled for BrUTP and UBF or for BrUTP and
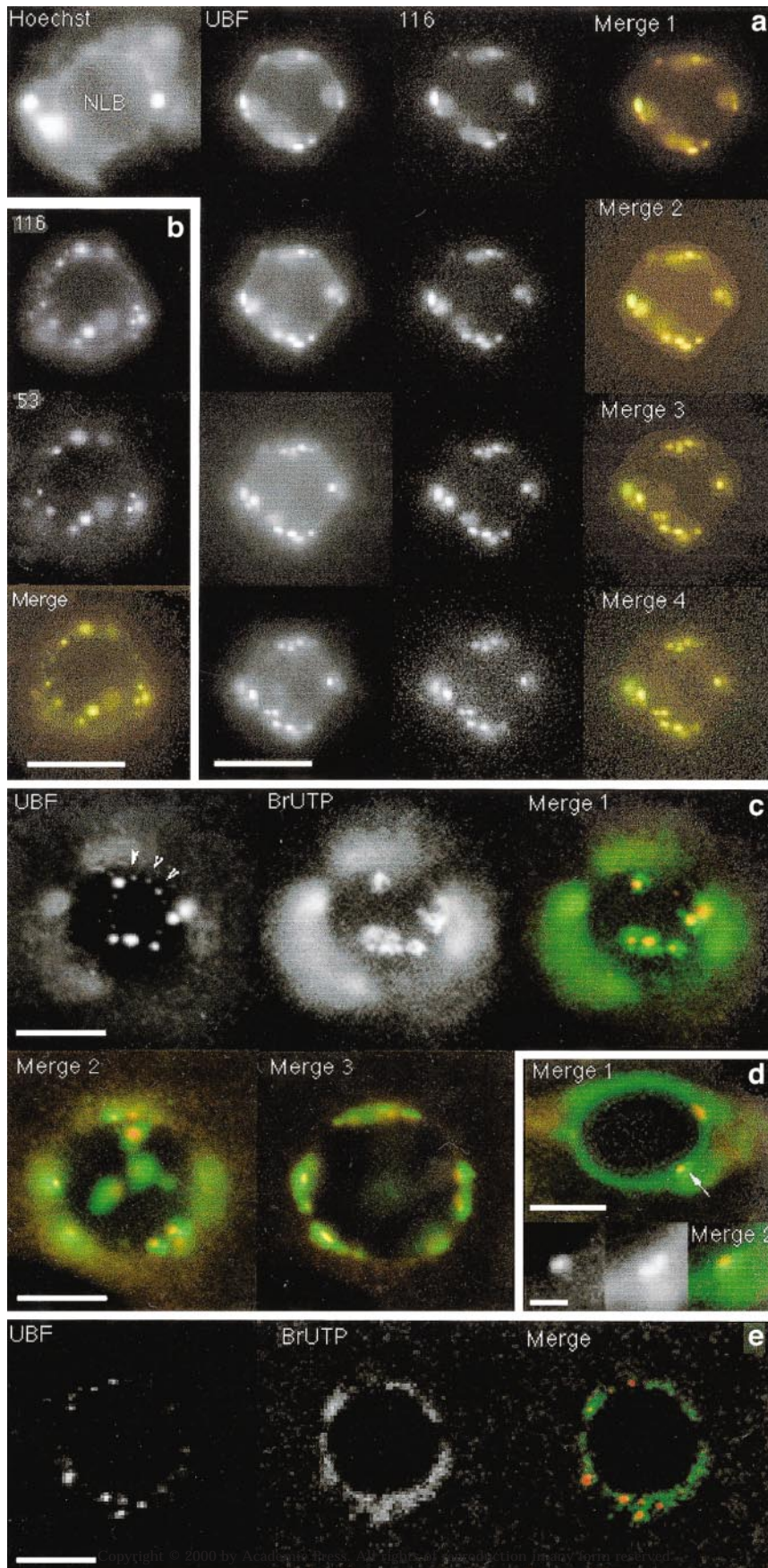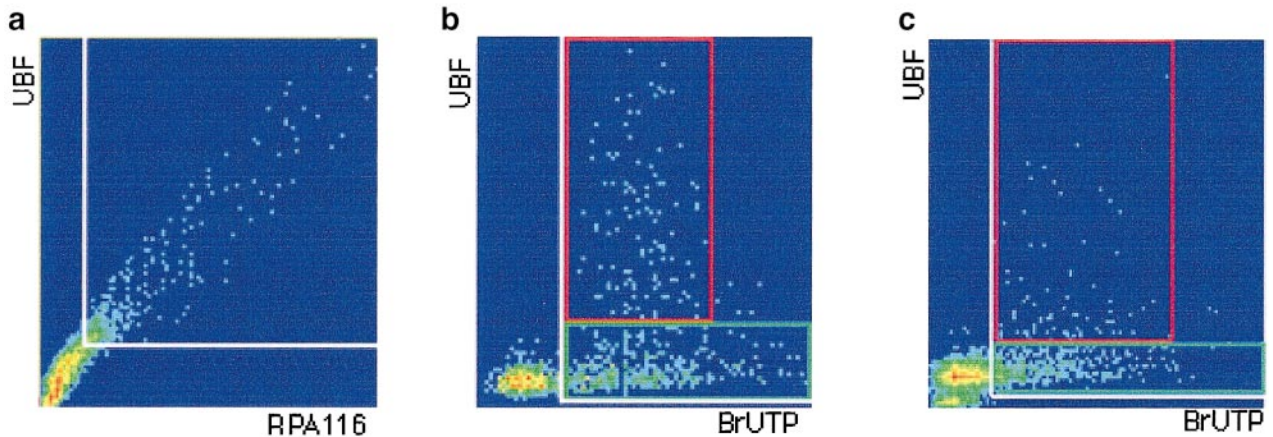
FIG. 3. SPIMAC analysis of conventional (a and b) and confocal (c) images of NSN oocytes shows a linear correlation between UBF and RPA116 intensities (a) and absence of such a correlation between UBF and transcription (b and c). The *x, y* coordinates of each point of the 2D histograms represent the normalized fluorescence intensity of a given pixel in UBF and RPA116 (or UBF and BrUTP) images, respectively. The two white lines separate the low-intensity pixels (background) from those specifically stained by both antibodies. In (a), data are obtained from the Merge 2 image of Fig. 2a. UBF and RPA116 intensities are correlated. In (b and c), data are taken from the Merge 1 image of Fig. 2c and Fig. 2e, respectively. UBF and BrUTP-tagged RNA are not correlated: pixels with high UBF content correspond to a low BrUTP labeling (red rectangle) while pixels of a high BrUTP labeling correspond to low UBF content (green rectangle).

RPA116, and examined with either a conventional (Fig. 2c) or a confocal microscope (Fig. 2e). As seen in these figures, newly synthesized rRNAs were spatially associated with UBF-positive foci but generally no BrUTP incorporation was observed inside large UBF foci per se (Fig. 2c, Merge 1–3). In addition, some minor UBF-binding sites were not associated with new transcripts (Fig. 2c, Merge 1). The SPIMAC analysis of the UBF/rRNA distribution further confirms these observations (Fig. 3b). The 2D histogram obtained from the couple of conventional images (Fig. 2c) reveals two populations of pixels: the first one (red rectangle on Fig. 3b) represents pixels in which all UBF labeling is concentrated; they have a low and nearly constant BrUTP content. The second population of pixels (green rectangle on Fig. 3b), in which all BrUTP labeling is concentrated, exhibits a low and constant UBF content. We obtained similar profiles of the 2D histograms for the confocal images of Fig. 2e (see Fig. 3c). This clearly demonstrates

that sites of high UBF and high BrUTP labeling are spatially separated. Similar results were obtained for BrUTP and RPA116 (not shown).

NLBs are composed of tightly packed material (Borsuk *et al.,* 1996; Masson *et al.,* 1996). We therefore questioned whether the exclusive perinucleolar location of the active rRNA transcription machinery observed in the *in toto* fixed oocytes could be caused by inaccessibility of the antibodies to the antigens hidden within the NLB mass. To test this, we prepared serial cryosections of BrUTP-microinjected oocytes and processed them for BrUTP and UBF immunolabeling. Remarkably, the pattern of oocyte labeling in sections was essentially similar to that following *in toto* immunolabeling (Fig. 2d). We therefore concluded that in transcriptionally competent NSN oocytes the RNA pol I machinery is associated solely with the NLB surface.

Then, we examined the molecular organization of early rRNA processing territories in combination with the rDNA

FIG. 2. In transcriptionally competent NSN oocytes, UBF and RPA116 (a) and RPA116 and PAF53/RPA53 (b) are distributed within the same discrete foci at the periphery of the NLB, whereas newly synthesized rRNAs are spatially associated but not completely overlapped with UBF (c and d). Isolated GV oocytes were microinjected with BrUTP, processed for immunolabeling with appropriate primary and secondary antibodies, and examined either with a conventional microscope (a–d) or with a confocal microscope (e) following partial squeezing of oocytes (c–e). Immunolabeling was performed either *in toto* (a, b, c, and e) or on cryosections (d). In (a), consequent optical sections of each immunolabeling and resulting merged image are shown. Hoechst 33342 DNA staining was used to assess the NSN type of chromatin configuration (a). In (a and c), separate UBF and BrUTP images are shown in black and white and merged images in color. In (c, d, and e), UBF is in red and BrU-rRNA in green. Arrowheads in (c), minor UBF-labeled foci that are excluded from ongoing transcription located at the surface of the NLB; arrow in (d), an active UBF-labeled site shown below at higher magnification in insets (Merge 2). Long bar, 10 μm. Short bar, 0.25 μm
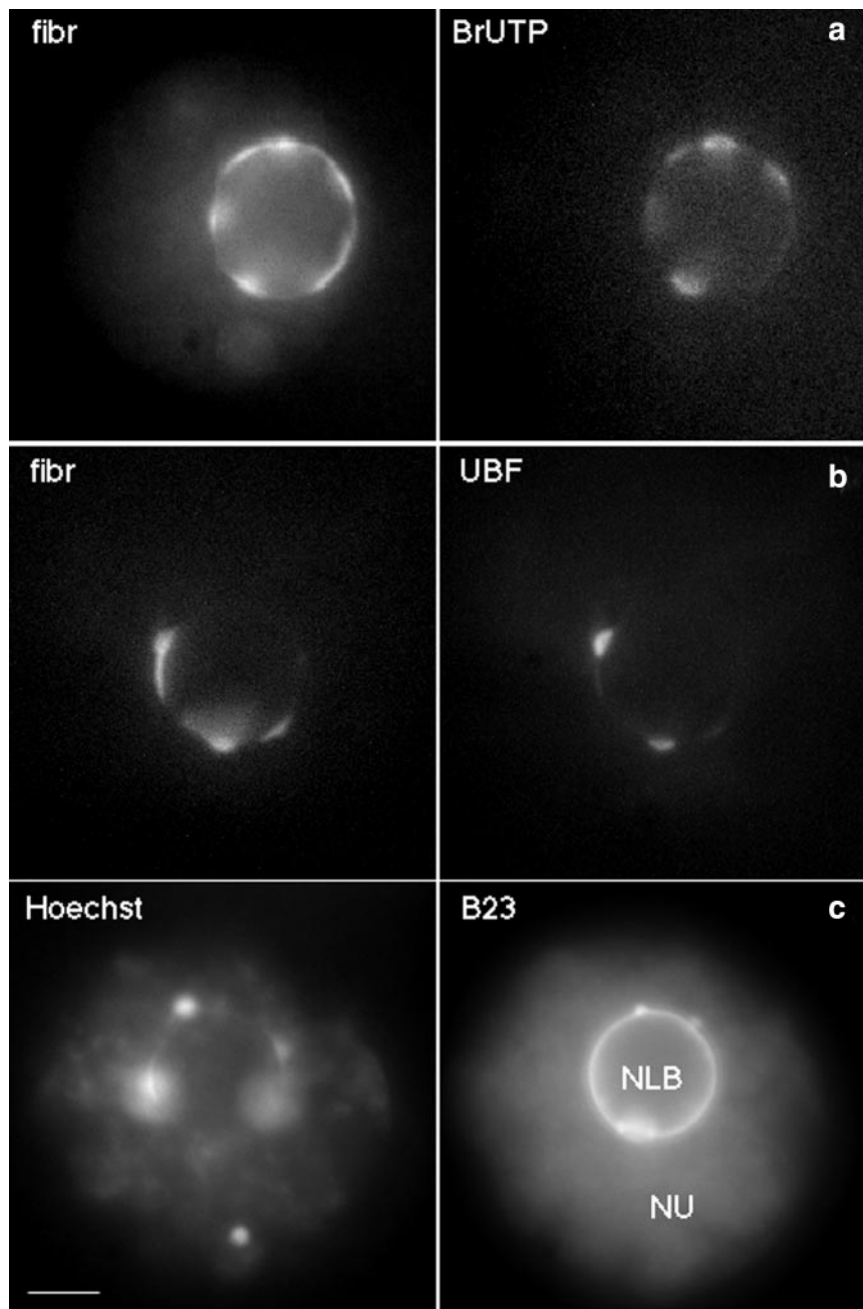
FIG. 4. In transcriptionally competent NSN oocytes, fibrillarin (fibr) is associated with the nucleolus-like body (NLB) periphery and is partially coincident with the newly synthesized rRNA (BrUTP) (a) and UBF (b); B23 protein is widely distributed over the NLB surface and in the nucleoplasm (NU) (c). Hoechst DNA staining illustrates the chromatin configuration. Bar, 10 μm.

transcription domains. For that, we immunolabeled mouse oocytes with antibodies against fibrillarin, an early pre-RNA processing protein marker, in parallel with BrUTP or UBF (Figs. 4a and 4b, respectively). As one can see in Fig. 4a, fibrillarin was located solely at the NLB surface. Its binding sites were coincident, but did not completely overlap, with

the nascent rRNA transcripts. A close association, but not entire overlapping, was also observed for fibrillarin and UBF (Fig. 4b). These results were further confirmed on cryosections of NSN oocyte (not shown). Unlike fibrillarin, B23 protein was distributed over the entire NLB surface. In addition, some B23 fluorescence was also observed in the
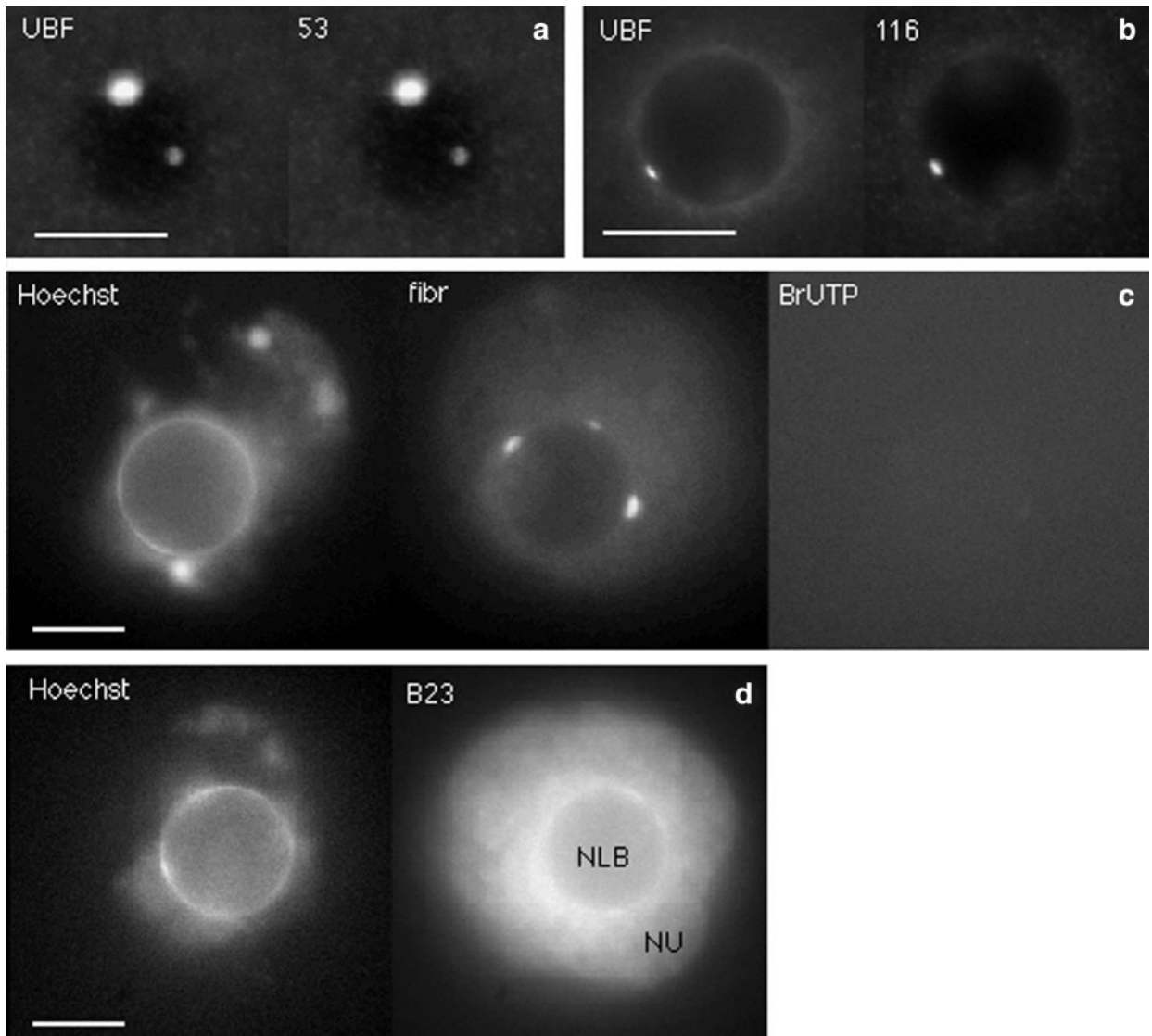
FIG. 5. In transcriptionally incompetent SN oocytes, UBF, PAF53/RPA53 (53), and RPA116 (116) remain bound to the NLB periphery and are perfectly colocalized (a and b); fibrillarin (fibr) is still associated with the NLB, even in the absence of ongoing rRNA synthesis (c, BrUTP); B23 protein is mainly localized in the nucleoplasm (NU). Hoechst 33342 staining shows a condensed perinucleolar chromatin ring (c and d). Bars, 10 μm.

nucleoplasm (Fig. 4c). Therefore, early rRNA processing proteins behave similarly in transcribing oocytes and in somatic cells (Garcia-Blanco *et al.,* 1995; Lazdins *et al.,* 1997).

The RNA Pol I Synthesis Machinery Remains Associated with NLBs in Transcriptionally Inert GV Oocytes

We next examined the behavior of RNA pol I transcriptional machinery in transcriptionally incompetent SN oocytes using the same experimental approaches as for NSN

oocytes (Fig. 5). Quite surprisingly, all the SN oocytes examined were positively labeled for UBF and RNA pol I (Figs. 5a and 5b), despite the fact that they did not incorporate BrUTP. Moreover, UBF, PAF53/RPA53, and RPA116 were associated with the NLB surface and were entirely coincident (Figs. 5a and 5b). Generally, the signals were observed in interruptions of the perinucleolar chromatin ring weakly stained by Hoechst 33342 (not shown). However, in comparison with the NSN-type GV oocytes, the total spot number was reduced to 3–5 per cell (Figs. 5a and 5b). SPIMAC analysis further showed that within these spots all the components of the RNA pol I transcriptional
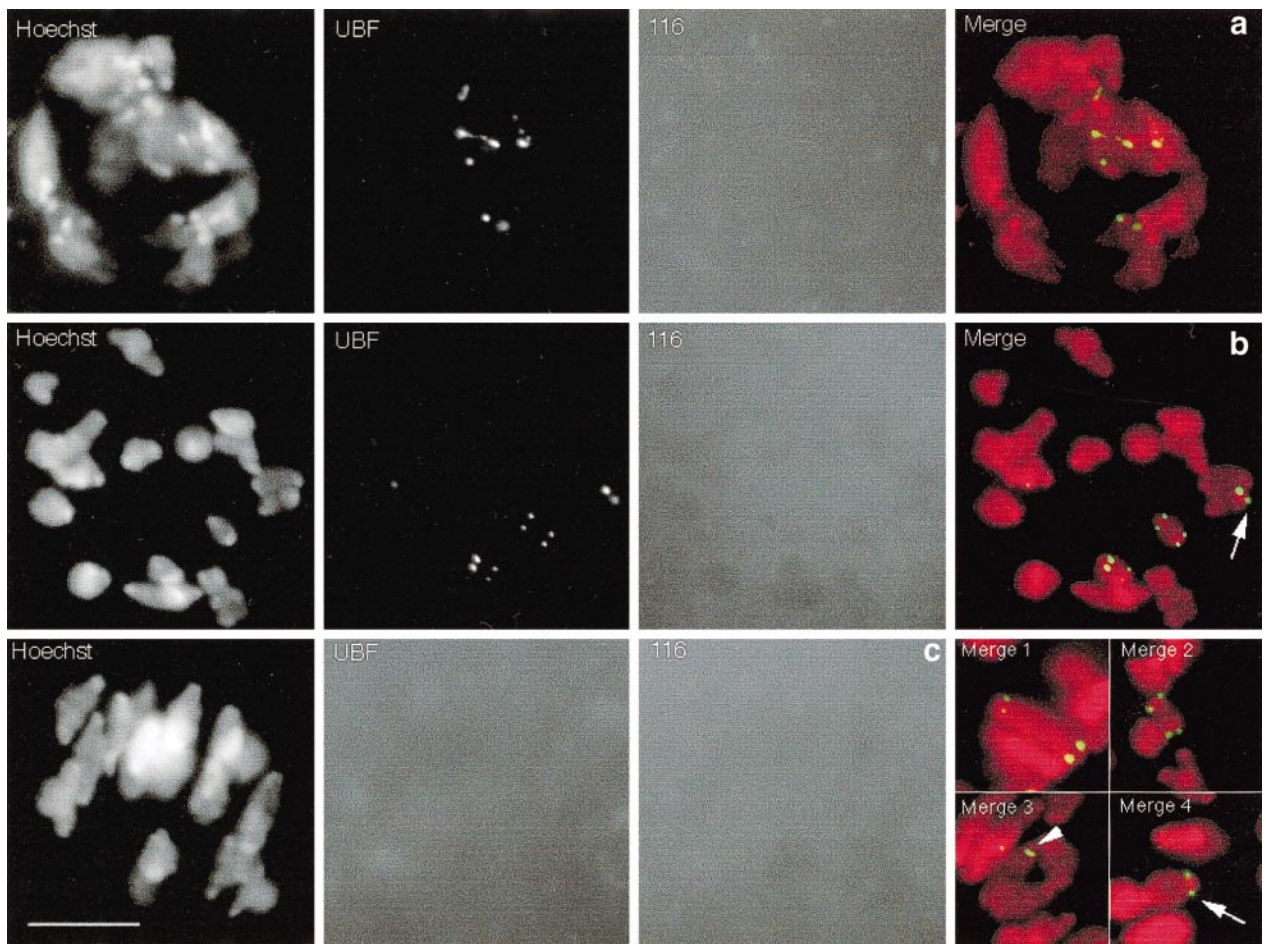
FIG. 6. During oocyte maturation, UBF remains bound to the meiotic chromosomes longer than RPA116 (116). Maturing oocytes were processed for double immunolabeling with anti-UBF and anti-RPA116 antibodies shortly after GVBD (a) or at 6 h (b, early/middle prometaphase I) and 9 h (c, late prometaphase I) postisolation. Merge images are shown in false colors, with UBF in green and chromosomes in red. Details of a few other examples of UBF-positive middle/late prometaphase I chromosomes are given in Merge 1 to 4. UBF signals are seen as single or double spots positioned nearby the centromeric heterochromatin. In a bivalent, homologous chromosomes can be labeled asymmetrically (arrows); in Merge 3, a chromosomal bivalent exhibiting a crescent shape structure is indicated by arrowhead. Bar, 10 μm.

machinery were present in a constant molar ratio (pixel-by-pixel fluorescence intensities correlated with $r = 0.93$ to 0.95, not shown), as in the case of transcribing NSN oocytes. Despite the lack of detectable transcription, fibrillarin was distributed in a few spots apposed to the nucleolar outline (Fig. 5c) and in part associated with UBF (not shown). As for the B23 protein, it was mainly located in the nucleoplasm of SN oocytes, and the perinucleolar B23 ring became less evident than in NSN oocytes (Figs. 5d and 4c).

Components of the rDNA Transcription Complex Dissociate Sequentially from the Chromosomes during Meiotic Divisions

Mouse oocytes resume spontaneously their meiotic maturation when released from follicles and cultured *in*

vitro (Donahue, 1968). We took advantage of these facts to examine in details the dynamics of the rDNA transcription complex and its interaction with chromosomes throughout progression to MII. Immunolabeling of oocytes at subsequent stages of the first meiotic division showed that RNA pol I subunits RPA116 and PAF53/RPA53 were no more detectable starting from early GVBD onward (Fig. 6a and results not shown). On the contrary, UBF was associated with chromosomes until the MI stage. In all oocytes fixed just at the moment of—or slightly after—the NLB dissolution that is the landmark of GVBD, UBF was found within several spots of various size and intensity decorating the chromosomes (Fig. 6a). Note that individual chromosomes can hardly be distinguished at that stage (Fig. 6a). Then, the number of UBF-positive oocytes declined gradually in par-
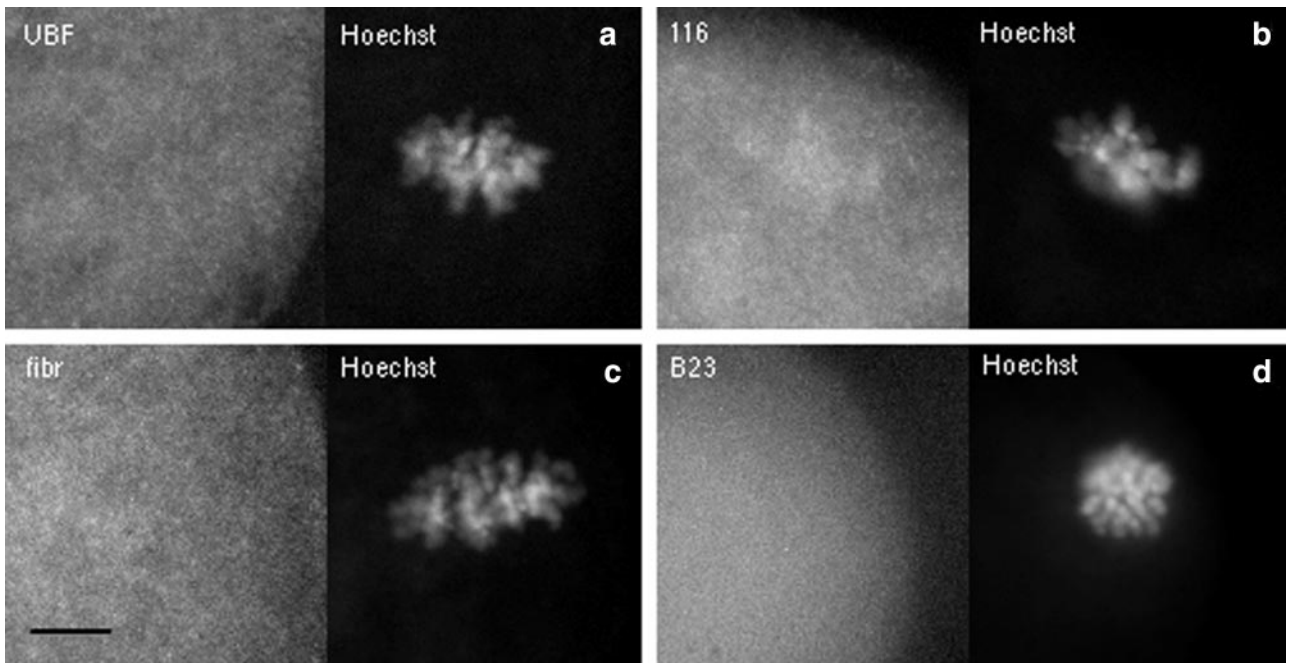
FIG. 7. Immunolabeling of chromosomes in MII oocytes is entirely negative for UBF (a), RPA116 (b), fibrillarin (c), and B23 (d). MII oocytes were isolated from ampullae, immunolabeled *in toto,* and stained with Hoechst 33342. Bar, 10 μm.

allel with chromosome condensation. Three hours after collection, when oocytes were at early prometaphase I (see Donahue, 1968; Debey *et al.,* 1993; for stage identification), about 90% of oocytes examined ($n = 33$) were labeled. Six hours after isolation (middle/late prometaphase), only 57% of oocytes ($n = 47$) contained UBF-positive chromosomes (Fig. 6b). This proportion dropped to 36% in the oocytes which were in late prometaphase stage at 9 h postisolation ($n = 39$) and no MI oocyte was labeled. At each time point, oocytes had a variable number of UBF-labeled bivalents, from 5 to 1. However, the proportion of oocytes with five labeled bivalents was practically constant: 56, 55, and 60% after 3, 6, and 9 h of culture, respectively (not significantly different values). The number of UBF spots per bivalent varied from 4, the expected number if UBF would bind all chromatids, to 1 (Fig. 6, see merged images). When a single UBF spot per bivalent was present, it had generally an elongated crescent-like shape (Fig. 6, see Merge 3). UBF signals were always located near the centromeric regions of chromosomes, which were recognized due to their preferential staining with Hoechst 33242.

Starting from MI onward all the oocytes were UBF and RPA116 negative (Fig. 6c). The same was also true for the *in vivo* matured MII oocytes whatever the fixation procedure (PFA or methanol) (Figs. 7a and 7b). Moreover, none of the rRNA processing proteins examined was observed in association with MI or MII chromosomes (Figs. 7c and 7d). Note that GV oocytes which were processed for immuno-

labeling simultaneously with MII oocytes as positive controls were always labeled.

UBF and RPA116 Are Degraded in MII Oocytes

The negative immunolabeling of MI and MII meiotic chromosomes for UBF and RNA pol I was unexpected, since these factors are known to bind the chromosomal NORs during mitosis (Zatsepina *et al.,* 1993; Seither *et al.,* 1997). To learn whether the loss of chromosomal labeling was due to protein degradation or was caused by their displacement to the cytoplasm, we performed Western blot analysis of total MII oocyte extracts. GV oocytes and NIH3T3 extracts were loaded in the same gels as positive controls. As shown in Fig. 1, RPA116 and UBF were readily recovered in extracts made from 100 (Figs. 1a and 1b) and 150 (Figs. 1c and 1d) GVs, but very weak (if any) signals were observed in MII extracts, even when they were prepared from 200 oocytes (Figs. 1c and 1d). These results indicate that oocyte progression to MII is accompanied by degradation of both RPA116 and UBF, a process which might largely contribute to the lack of MII chromosome labeling.

UBF Interaction with Meiotic Chromosomes Depends on Protein Phosphorylation

In somatic cells, the phosphorylation/dephosphorylation status regulates in a complex manner the interaction between proteins of the transcription complex, particularly at

the preinitiation step (O'Machony *et al.,* 1992; Voit *et al.,* 1992, 1999; Labhart, 1994; Heix *et al.,* 1998; Kihm *et al.,* 1998). On the other hand, progression through meiosis rests on a specific pattern of kinases and phosphatases activation (Verlhac *et al.,* 1994; Murray, 1998, Winston and Maro, 1999). We therefore addressed the question of whether the binding of UBF and RPA116 to meiotic chromosomes would be altered by phosphatase or kinase inhibitors. Exposure of GVBD oocytes to the general kinase inhibitor 6-DMAP did not significantly affect the pattern and dynamics of chromosome labeling by UBF (Fig. 8a). The number of oocytes labeled decreased similar to that of untreated controls (Fig. 8b), and based on the Student test the difference between the control and the 6-DMAP values was not significant. A profound effect, however, was achieved by the potent type-1 and -2A phosphatase inhibitor OA, which impaired UBF detachment from the chromosomes for more than 9 h (Fig. 8b). It was noteworthy that neither drug impaired the RNA pol I dissociation from chromosomes at GVBD (data not shown). Altogether these results favor the idea that detachment of UBF—but not of RNA pol I—from meiotic chromosomes is regulated by a protein phosphorylation balance.

DISCUSSION

This work is the first concerning the fate of key components of the rRNA synthesis and processing machineries in fully grown GV mouse oocytes throughout meiotic maturation and in relation to the ongoing rDNA transcription. The main results are summarized in Fig. 9. They show a tight relationship between the rRNA transcription machinery and the subnuclear compartment known as "NLB" in fully grown oocytes and reveal distinct dynamics of nucleolar components in meiosis and mitosis.

In Fully Grown Mouse GV Oocytes, the RNA Pol I Machinery Remains Present at the NLB Surface Whatever Their Transcriptional Activity

The unusual ultrastructure of the NLBs of fully grown mammalian oocytes was recognized a long time ago (Chouinard, 1971; Mirre and Stahl, 1981). They are composed of tightly packed fibrous material and apparently lack the characteristic features attributed to nucleoli of actively transcribing somatic cells, such as fibrillar centers and the dense fibrillar component, which are known to be the major locations for RNA pol I and UBF (reviewed by Hadjiolov, 1985; Shaw and Jordan, 1995). Nevertheless, transcriptional activity was demonstrated in fully grown GV oocytes of NSN type, as was, at the ultrastructural level, the presence of intra-NLB vacuoles and peri-NLB protrusions of fibrillogranular material (Debey *et al.,* 1993; Borsuk *et al.,* 1996; Bouniol-Baly *et al.,* 1999). Here we show that, in this class of oocyte, three ubiquitous members of the RNA pol I transcription complex, namely UBF, RPA116, and PAF53/

RPA53, remain present. They are distributed between numerous discrete foci associated solely with the NLB surface. These UBF/RNA pol I foci are often organized as necklaces separated by regular intervals of about 1 μm which could represent, as in somatic cells, single rDNA repeats interrupted by intergenic spacers in a rather extended DNA configuration (Scheer *et al.,* 1984; Haaf *et al.,* 1991; Le Panse *et al.,* 1999). In addition, RPA116, PAF53/RPA53, and UBF seem to be present in these foci with a constant stoichiometry. Although RPA116 and PAF53/RPA53 have been proposed to have different RNA pol I complex-binding properties in mouse fibroblasts (Hanada *et al.,* 1996), in oocytes they appear to behave in a similar manner. Moreover, the nascent BrU–rRNAs are spatially associated with the RNA pol I complex/UBF and overlap partly with the rRNA processing territories containing fibrillarin, as it is characteristic of somatic cells. The small UBF/pol I foci not associated with transcription (Fig. 2c) could represent clusters of inactive rRNA genes which may exist in somatic cells also (Junera *et al.,* 1997). Thus, altogether, our data favor the idea that the basic bipartite organization of the rRNA synthesis and processing domains (Garcia-Blanco *et al.,* 1995; Lazdins *et al.,* 1997) is maintained in fully grown oocytes despite striking differences in the nucleolar architecture between somatic and germinal cells.

We found that the down-regulation of rDNA transcription in SN-type GV oocytes was not associated with physical detachment of the RNA pol I transcription complex from its binding sites (the NLB surface), but with a reduction in the number and an increase in the size of the foci (Fig. 5). A similar trend was already observed in serum-deprived somatic cells (Zatsepina *et al.;* 1993; Seither *et al.,* 1997) or following actinomycin D treatment, which inhibits its rRNA synthesis. The latter causes redistribution of rDNA templates in a few large perinucleolar clusters, which retain the major components of the transcription machinery (Jordan *et al.,* 1996). By analogy, one could propose that the physiological block of transcription that accompanies transformation of the NSN into the SN chromatin configuration is linked to a clustering of the rDNA-encoding genes and their associated proteins. We observed that the large UBF/pol I foci found in inactive SN-type GV oocytes are located preferentially in perinuclear zones that are more weakly stained by Hoechst than the intensely stained perinucleolar chromatin ring. However, this does not reveal whether the proteins are bound to rDNA or clustered in purely protein/protein complexes. *In situ* hybridization should allow this question to be resolved. Finally, the down-regulation of ribosomal transcription is accompanied by dispersion of B23 into the nucleoplasm. Nevertheless, it remains clear that in fully grown mouse oocytes no visible amounts of key nucleolar protein, such as UBF, RNA pol I, fibrillarin, or B23, are accumulated within the NLB interior, and only their surface serves as a "structural" support for the rDNA transcription and early rRNA processing events.
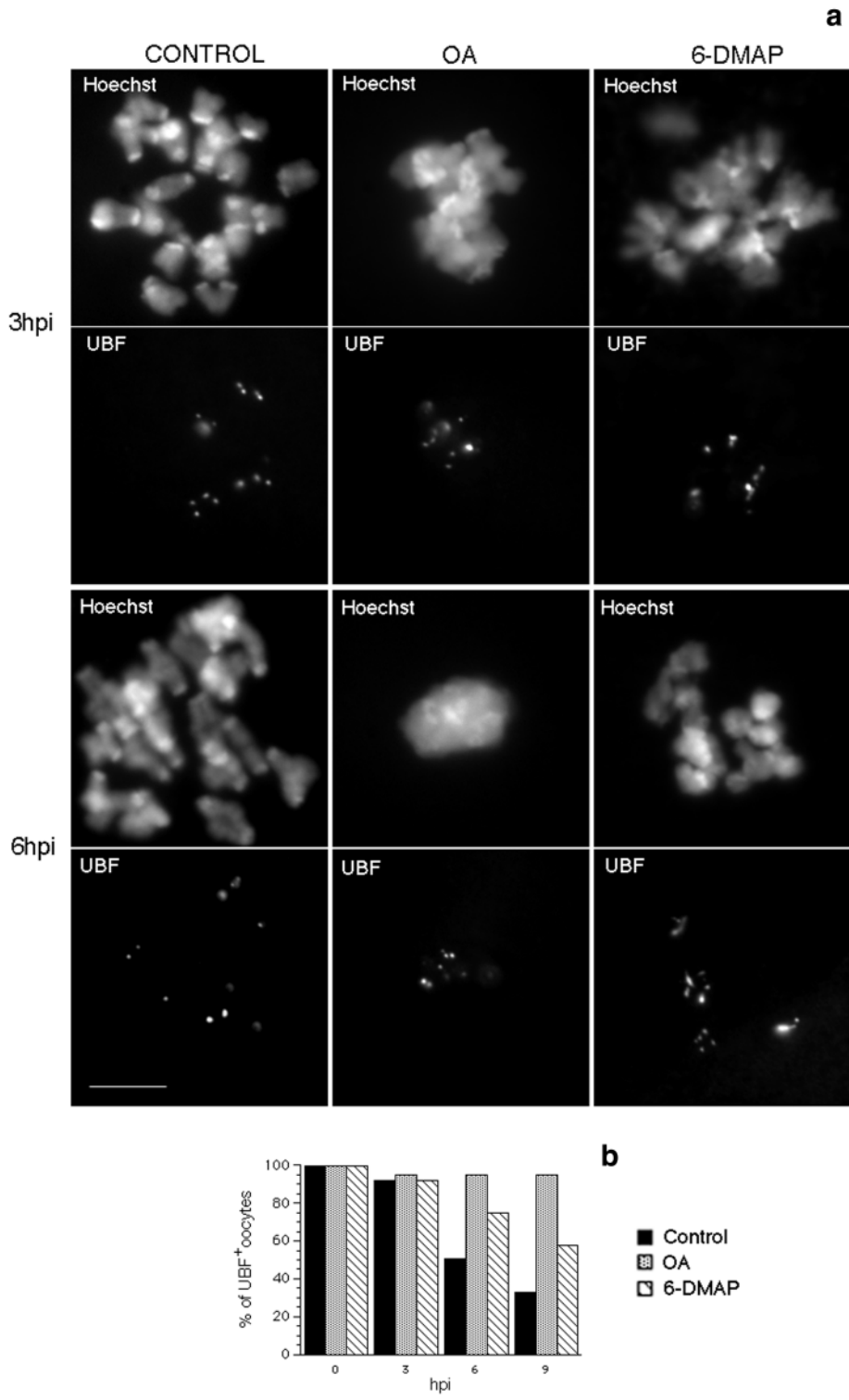
FIG. 8. General view (a) and percentage (b) of UBF-positive oocytes observed in control (CONTROL) or in the presence of 1 μM okadaic acid (OA) or 2.5 mM 6-DMAP (6-DMAP) at 3, 6, and 9 h postisolation (hpi). See Materials and Methods for the protocols. For each point, 20 to 40 oocytes were examined. Bar, 10 μm.
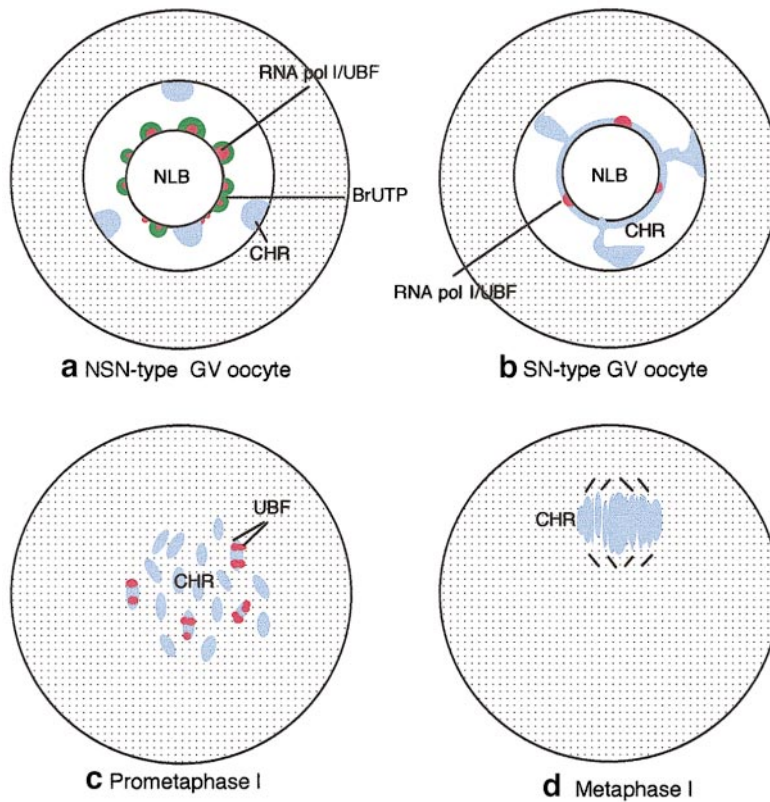
FIG. 9. Scheme illustrating the status of the of the RNA pol I transcription complex in a transcriptionally competent NSN oocyte (a), in a transcriptionally incompetent SN oocyte (b), and at the early prometaphase I (c) and metaphase I (d) stages. NLB, nucleolus like body; BrUTP, nascent rRNAs; RNA pol I/UBF, rDNA transcription complex consisting of RNA pol I and UBF; CHR, chromatin and chromosomes. Cessation of rRNA synthesis is not correlated with the physical detachment of the RNA pol I transcriptional machinery from the rDNAs, but occurs after the GV dissolution, during prometaphase I. Neither component of the rDNA transcription complex is associated with the MI chromosomes (d).

The RNA Pol I Machinery Dissociates in a Stepwise Manner from Chromosomes during Progression through Meiosis

Surprisingly and in contrast to any known events that occur during mitosis, progression of oocytes through meiosis is accompanied by progressive dislodging of the RNA pol I machinery from its binding sites and, starting from MI onward, neither RNA pol I nor UBF could be detected over the chromosomes, although they are readily detected on mitotic chromosomes of cycling cells (Zatsepina *et al.,* 1993; Roussel *et al.,* 1996). These data are consistent with previous observations that chromosomal NORs, which are Ag-positive during the whole meiotic prophase I, become Ag-negative in MI and MII oocytes as well as during interkinesis (Engel *et al.,* 1977; Hansmann *et al.,* 1978; Amikura *et al.,* 1987; Dyban *et al.,* 1988). Since in somatic cells, the silver-binding capacity of chromosomal NORs reflects the specific affinity of RNA pol I and UBF for silver ions (Roussel and Hernandez-Verdun, 1994), our results

indicate that RNA pol I and/or UBF are Ag-binding proteins of the chromosomal NORs at meiosis as well.

In addition, much less UBF and RPA116 were recovered in the total protein extracts prepared from MII oocytes compared with GV oocytes (Figs. 1c and 1d). This fact indicates a degradation of the RNA pol I transcription complexes at MII. Whether this degradation is caused by or leads to the dissociation of the complexes from the rDNAs remains to be established (see below). It has been shown recently that in mammals part of RNA pol I can exist as "holoenzyme" that contains basal transcription (TIF-IA, TIF-IB/SL1, UBF) and termination (TTF-1) factors, but does not interact with the ribosomal genes directly (Seither *et al.,* 1998; Hannan *et al.,* 1999). One could speculate therefore that the faint anti-UBF and anti-RPA116 signals observed in mouse MII extracts by Western blots might be produced by rDNA-unbound ("free") RNA pol I holoenzymes.

Neither RPA116 nor PAF53/RPA53 can be observed in

oocytes at early GVBD stage, while UBF is maintained on chromosomes until metaphase I, i.e., about 8–9 h longer. Such disjunction of UBF and RNA pol I behavior does not result from the procedure of oocyte fixation, since both PFA and methanol provide similar results, and is also not a unique case. It was recently demonstrated in *Xenopus* oocyte extracts *in vitro* (Bell *et al.,* 1997) or in transcriptionally inert *Xenopus* embryos *in situ* (Verheggen *et al.,* 1998) that UBF can interact with nontranscribed rDNA prior to other components of the RNA pol I transcription machinery, such as TBP and RNA pol I. It was thus assumed that UBF has a higher affinity to the NORs than other nucleolar proteins and may play the role of an architectural element that converts the rDNA chromatin into a transcriptionally competent form (Bell *et al.,* 1997). The kinetics of the RNA transcription complex disassembly during the first meiotic divisions in mouse oocytes is entirely consistent with this assumption.

Currently, we have no direct evidence that UBF specifically binds the NORs rather than other regions of the chromosomes in transcriptionally silent SN-type GV oocytes and after GVBD. However, the pattern of chromosomal labeling strongly argues in favor of specific UBF–rDNA interactions: (1) UBF was systematically revealed within double or single fluorescence spots located close to the centromeric heterochromatin, where the chromosomal NORs are known to be located in the mouse (Elsevier and Ruddle, 1975); (2) the maximal number of UBF spots per bivalent was 4, i.e., one spot per chromatid; (3) the total number of UBF-positive bivalents per oocyte, no more than 5, did not exceed that of the NORs-bearing chromosomes in mouse strains (up to 6 for a haploid set of chromosomes; Winking *et al.,* 1980). Based on these arguments, we believe that UBF remains specifically bound to the ribosomal genes until its dissociation from chromosomes. However, at any stage between GVBD and MI, half of UBF-positive oocytes have fewer than five chromosomes labeled. It can therefore be suggested that, as in somatic cells (Roussel *et al.,* 1996; Heliot *et al.,* 1997), not all NORs are actively transcribed in oocytes at the preceding GV stages. An asymmetric labeling of homologous chromosomes for UBF also favors this view (Fig. 6).

What might be the mechanism(s) that causes RNA pol I and UBF dissociation from the prometaphase I chromosome? In somatic cells, two members of the RNA pol I machinery, UBF and SL1, are the main targets for cell-cycle-dependent kinases (Heix *et al.,* 1998; Kihm *et al.,* 1998; Voit *et al.,* 1999). During interphase, the regulation of UBF activity by phosphorylation through cell-cycle kinases appears quite complex (O'Machony *et al.,* 1992; Voit *et al.,* 1992, 1999). At mitosis, UBF and SL1 are both inactivated by phosphorylation through M-phase-associated kinases (Heix *et al.,* 1998; Klein and Grummt, 1999), although the rDNA-binding capacity of UBF is not impaired (Roussel *et al.,* 1996) and seems even enhanced compared to interphase (Sirri *et al.,* 1999). It was therefore surprising to observe detachment of UBF from chromosomes during meiotic

maturation, i.e., in a context of high activity of kinases, such as p34cdc2 and MAP kinase (Gavin *et al.,* 1992; Chesnel and Eppig, 1995; Verlhac *et al.,* 1994; Murray, 1998). Actually, UBF detachment is not abrupt (90% of oocytes are still labeled after 3 h of culture), which suggests that it could be linked to molecular processes occurring after the initial rise in kinase activity. The overall period from early prophase to metaphase I is unusually long-lasting. It is characterized by a sustained increase of MAP kinase and p34cdc2 activities (Verlhac *et al.,* 1994) and a sharp increase, followed by a progressive decline, in the activity of PP2A, which is a target for OA (Winston and Maro, 1999). The fact that UBF detachment from meiotic chromosomes is impaired by OA but not affected by 6-DMAP suggests that this process is linked to a progressive decrease of the overall phosphorylation level as meiosis progresses. Actually, we do not know whether OA affects directly the phosphorylation level of UBF or acts indirectly, for example via the modulation of the interaction of UBF with other UBF binding proteins, like SL1 and its counterparts, or yet by modifying the protein turnover (see above). It is worth noting, however, that RPA116 and PAF53/RPA53 dissociate abruptly from the chromosomes at early GVBD and that this process is not affected by changes in the phosphorylation/dephosphorylation balance.

In addition to RNA pol I and UBF, fibrillarin and B23 were not associated with MI and MII chromosomes, despite the fact that both proteins are found at the periphery of chromosomes in mitotic cells (Jimenez-Garcia *et al.,* 1994; Weisenberger and Scheer, 1995; Zatsepina *et al.,* 1997; Magoulas *et al.,* 1998). Thus, none of the nucleolar proteins involved either in the rDNA transcription (UBF, RPA116, and PAF53/RPA53) or in early rRNA processing (fibrillarin) or yet in assembly of mature preribosomal particles (B23) is apparently transported to zygotes by the maternal chromosomes.

In conclusion, despite an extraordinary difference in the ultrastructure of NLBs in GV oocytes compared to nucleoli of cycling somatic cells, the molecular organizations of the rRNA synthesis and processing machineries appear largely similar in both systems. Fundamental differences, however, are observed starting from GVBD onward. Different—or additional—mechanisms lead to the apparent degradation of major rDNA transcription complexes and/or their displacement from their targets, thus imposing a reliable additional rDNA arrest during meiotic divisions. Reactivation of rDNA transcription in fertilized zygotes will therefore require *de novo* assembly of the pol I-dependent initiation complex and its *de novo* interactions with the rDNA templates. In early embryos, RNA pol I-driven transcription starts later than the pol II-dependent transcription (Telford *et al.,* 1990; Verheggen *et al.,* 1998; and refs therein). The biological importance of a specific control of pol I-dependent transcription at the beginning of development may be approached through several models, including nuclear transfer.

ACKNOWLEDGMENTS

REFERENCES

Amikura, R. M., Yamada, H., Hirai, S., and Nagano, H. (1987). Intracellular localization of argyrophilic proteins in the maturing oocyte, fertilized egg, and spermatozoa of the starfish, Asterina pectinifera. *Gamete Res.* **16,** 291–301.

Amirand, C., Viari, A., Ballini, J.-P., Rezaei, H., Beaujean, N., Jullien, D., Käs, E., and Debey, P. (1998). Three distinct subnuclear populations of HMG-I protein of different properties revealed by co-localization image analysis. *J. Cell Sci.* **111,** 3551–3651.

Antoine, N., Lepoint, A., Baeckeland, E., and Goessens, G. (1988). Ultrastructural cytochemistry of the nucleolus in rat oocytes at the end of the folliculogenesis. *Histochemistry* **89,** 221–226.

Antoine, N., Thiry, M., and Goessens, G. (1989). Ultrastructural and cytochemical studies on extranucleolar bodies in rat oocytes at preovulatory follicle stage. *Biol. Cell* **65,** 61–66.

Bazett-Jones, D. P., Lablane, M., Herfort, M., and Moss, T. (1994). Short-range DNA looping by the Xenopus HMG-box transcription factor, xUBF. *Science* **264,** 1134–1137.

Bell, P., Mais, C., McStay, B., and Scheer, U. (1997). Association of the nucleolar transcription factor UBF with transcriptionally inactive rRNA genes of pronuclei and early Xenopus embryos. *J. Cell Sci.* **110,** 2053–2063.

Bloom, A. M., and Mukherjee, B. B. (1972). RNA synthesis in maturing mouse oocytes. *Exp. Cell Res.* **74,** 577–582.

Borsuk, E., Szöllösi, M. S., Besombes, D., and Debey, P. (1996). Fusion with activated mouse oocytes modulates the transcriptional activity of introduced somatic cell nuclei. *Exp. Cell Res.* **225,** 93–101.

Bouniol-Baly, C., Nguyen, E., Besombes, D., and Debey, D. (1997). Dynamic organization of DNA replication in one-cell mouse embryos: Relationship to transcriptional activity. *Exp. Cell Res.* **236,** 201–211.

Bouniol-Baly, C., Hamraoui, L., Guibert, J., Beaujean, N., Szöllösi, M. S., and Debey, P. (1999). Differential transcriptional activity associated to chromatin configuration in fully grown GV mouse oocytes. *Biol. Reprod.* **60,** 580–587.

Chesnel, F., and Eppig, J. J. (1995). Synthesis and accumulation of p34cdc2 and cyclin B in mouse oocytes during acquisition of competence to resume meiosis. *Mol. Reprod. Dev.* **40,** 503–508.

Chouinard, L. A. (1971). A light and electron-microscopy study of the nucleolus during growth of the oocyte in the prepubertal mouse. *J. Cell Sci.* **9,** 637–663.

Crozet, N. (1989). Nucleolar structure and RNA synthesis in mammalian oocytes. *J. Reprod. Fertil.* **38,** 9–16.

Debey, P., Szöllösi, M. S., Szöllösi, D., Vautier, D., Girousse, A., and Besombes, D. (1993). Competent mouse oocytes isolated from antral follicles exhibit different chromatin organization and follow different maturation dynamics. *Mol. Reprod. Dev.* **36,** 59–74.

Donahue, R. P. (1968). Maturation of the mouse oocyte in vitro. I. Sequence and timing of nuclear progression. *J. Exp. Zool.* **169,** 237–250.

Dyban, A. P., Lee, K., O'Neill, G. T., Speirs, S., and Kaufman, M. H. (1988). Cytogenetic study of silver-staining NORs in 8-cell-stage mouse blastomeres fused to 1-cell-stage embryos. *Development* **104,** 453–463.

Elsevier, S. M., and Ruddle, F. H. (1975). Localisation of genes coding for 18S and 28S ribosomal RNA within the genome of Mus musculus. *Chromosoma* **52,** 219–228.

Engel, W., Zenzes, M. T., and Schmid, M. (1977). Activation of mouse ribosomal RNA genes at the 2-cell stage. *Hum. Genet.* **38,** 57–63.

Fulton, B. P., and Whittingham, D. S. G. (1978). Activation of mammalian oocytes by intracellular injection of calcium. *Nature* **273,** 149–151.

Garcia-Blanco, M. A., Miller, D. D., and Sheetz, M. P. (1995). Nuclear spreads. I. Visualization of bipartite ribosomal RNA domains. *J. Cell Biol.* **128,** 15–27.

Gavin, A.-C., Vassalli, J.-D., Cavadore, J. C., and Schorderet-Slatkine, S. (1992). Okadaic acid and p13suc1 modulate the reinitiation of meiosis in mouse oocytes. *Mol. Reprod. Dev.* **33,** 287–296.

Haaf, T., Hayman, D. L., and Schmid, D. L. (1991). Quantitative determination of rDNA transcription units in vertebrate cells. *Exp. Cell Res.* **193,** 78–86.

Hadjiolov, A. A. (1985). "The Nucleolus and Ribosome Biogenesis," pp. 1–128. Springer-Verlag, Vienna, New York.

Hanada, K., Song, C. Z., Yamamoto, K., Yano, K., Maeda, Y., Yamaguchi, K., and Muramatsu, M. (1996). RNA polymerase I associated factor 53 binds to the nucleolar transcription factor UBF and functions in specific rDNA transcription. *EMBO J.* **15,** 2217–2226.

Hannan, R. D., Cavanaugh, A., Hempel, W. M., Moss, T., and Rothblum, L. (1999). Identification of a mammalian RNA polymerase I holoenzyme containing components of the DNA repair/replication system. *Nucleic Acids Res.* **27,** 3720–3727.

Hansmann, I., Gebauer, J., Bihl, L., and Grimm, T. (1978). Onset of nucleolus organizer activity in early mouse embryogenesis and evidence for its regulation. *Exp. Cell Res.* **114,** 263–268.

Heix, J., Vente, A., Voit, R., Budde, A., Michaelidis, T. M., and Grummt, I. (1998). Mitotic silencing of human rRNA synthesis: Inactivation of the promoter selectivity factor SL1 by cdc2/cyclin B-mediated phosphorylation. *EMBO J.* **17,** 7373–7381.

Heliot, L., Kaplan, H., Lucas, H., Klein, C., Beorchia, A., Doco-Fenzy, M., Menager, M., Thiry, M., O'Donahue, M. F., and Ploton, D. (1997). Electron tomography of metaphase nucleolar organizer regions: Evidence for a twisted-loop organization. *Mol. Biol. Cell* **8,** 2199–2216.

Hernandez, N. (1993). TBP, a universal eukaryotic transcription factor? *Genes Dev.* **7,** 1291–1308.

Hubbel, M. R. (1985). Silver staining as an indicator of active ribosomal genes. *Stain. Techn.* **60,** 285–294.

Jantzen, H.-M., Admon, A., Bell, S., and Tjian, R. (1990). Nucleolar transcription factor hUBF contains a DNA-binding motif with homology to HMG proteins. *Nature* **344,** 830–836.

Jimenez-Garcia, L. F., Segura-Valdez, M., Ochs, R. M., Rothblum, L. I., Hannan, R., and Spector, D. L. (1994). Nucleologenesis: U3 snRNA-containing prenucleolar bodies move to sites of active pre-rRNA transcription after mitosis. *Mol. Biol. Cell* **5,** 955–966.

Jordan, P., Mannervik, M., Tora, L., and Carmo-Fonseca, M. (1996). In vivo evidence that TATA-binding protein/SL1 colocalizes with UBF and RNA polymerase I when rRNA synthesis is either active or inactive. *J. Cell Biol.* **133,** 225–234.

Junera, H. R., Masson, C., Geraud, G., Suja, J., and Hernandez-Verdun, D. (1997). Involvement of in situ conformation of ribosomal genes and selective distribution of upstream binding factor in rRNA transcription. *Mol. Biol. Cell* **8,** 145–156.

Kaplan, G., Abreu, S. L., and Bachvarova, R. (1982). rRNA accumulation and protein synthetic patterns in growing mouse oocytes. *J. Exp. Zool.* **220,** 361–370.

Kihm, A. J., Hershey, J. C., Haystead, T. A., Madsen, C. S., and Owens, G. K. (1998). Phosphorylation of the rRNA transcription factor upstream binding factor promotes its association with TATA binding protein. *Proc. Natl. Acad. Sci. USA* **95,** 14816–14820.

Klein, J., and Grummt, I. (1999). Cell cycle-dependent regulation of RNA polymerase I transcription: The nucleolar transcription factor UBF is inactive in mitosis and early G1. *Proc. Natl. Acad. Sci. USA* **96,** 6096–6101.

Kopecny, V., Landa, V., and Pavlok, A. (1995). Localization of nucleic acids in the nucleoli of oocytes and early embryos of mouse and hamster: An autoradiographic study. *Mol. Reprod. Dev.* **41,** 449–458.

Kopecny, V., Biggiogera, M., Laurincik, J., Pivko, J., Grafenau, P., Martin, T. E., Fu, X. D., and Fakan, S. (1996). Fine structural cytochemical and immunocytochemical analysis of nucleic acids and ribonucleoprotein distribution in nuclei of pig oocytes and early preimplantation embryos. *Chromosoma* **104,** 561–574.

Labhart, P. (1994). Identification of two steps during Xenopus ribosomal gene transcription that are sensitive to protein phosphorylation. *Mol. Cell Biol.* **14,** 2011–2020.

Laemmli, U. K. (1970). Cleavage of structural proteins during the assembly of the head of bacteriophage T4. *Nature* **15,** 680–685.

Lazdins, I. B., Delannoy, M., and Sollner-Webb, B. (1997). Analysis of nucleolar transcription and processing domains and pre-rRNA movements by in situ hybridization. *Chromosoma* **105,** 481–495.

Le Panse, S., Masson, C., Heliot, L., Chassery, J. M., Junera, H. R., and Hernandez-Verdun, D. (1999). 3-D organization of ribosomal transcription units after DRB inhibition of RNA polymerase II transcription. *J. Cell Sci.* **112,** 2145–2154.

Magoulas, C., Zatsepina, O. V., Jordan, P. W. H., Jordan, E. G., and Fried, M. (1998). The SURF-6 protein is a component of the nucleolar matrix and has a high binding capacity for nucleic acids in vitro. *Eur. J. Cell Biol.* **75,** 144–183.

Masson, C., Bouniol, C., Fomproix, N., Szöllösi, M. S., Debey, P., and Hernandez-Verdun, D. (1996). Conditions favoring RNA polymerase I transcription in permeabilized cells. *Exp. Cell Res.* **226,** 114–125.

Mattson, B. A., and Albertini, D. F. (1990). Oogenesis: Chromatin and microtubule dynamics during meiotic prophase. *Mol. Reprod. Dev.* **25,** 374–383.

Mirre, C., and Stahl, A. (1981). Ultrastructural organization, sites of transcription and distribution of fibrillar centres in the nucleolus of the mouse oocytes. *J. Cell Sci.* **48,** 105–126.

Moore, G. P. M., Lintern-Moore, S., Peters, H., and Faber, M. (1974). RNA synthesis in the mouse oocyte. *J. Cell Biol.* **60,** 416–422.

Murray, A. W. (1998). MAP kinases in meiosis. *Cell* **92,** 157–159.

Ochs, R. L., and Press, R. I. (1992). Centromere autoantigens are associated with the nucleolus. *Exp. Cell Res.* **200,** 339–350.

O'Machony, D. J., Xie, W. Q., Smith, S. D., Singer, H. A., and Rothblum, L. I. (1992). Differential phosphorylation and localization of the transcriptional factor UBF in vivo in response to serum deprivation. *J. Biol. Chem.* **267,** 35–38.

Prather, R., Simerly, C., Schatten, G., Pilch, D. R., Lobo, S. M., Marzluff, W. F., Dean, W. L., and Schultz, G. A. (1990). U3snRNP and nucleolar development during oocyte maturation, fertilization and early embryogenesis in the mouse: U3snRNA and snRNPs are not regulated coordinate with other snRNAs and snRNPs. *Dev. Biol.* **138,** 247–255.

Reeder, R. H., Pikaard, C. S., and McStay, B. (1995). UBF, an architectural element for RNA polymerase I promoters. *Nucleic Acids Mol. Biol.* **9,** 251–263.

Rodman, T. C., and Bachvarova, R. (1976). RNA synthesis in preovulatory mouse oocytes. *J. Cell Biol.* **70,** 251–257.

Roussel, P., and Hernandez-Verdun, D. (1994). Identification of Ag-NOR proteins, markers of proliferation related to ribosomal gene activity. *Exp. Cell Res.* **214,** 465–472.

Roussel, P., Andre, C., Comai, L., and Hernandez-Verdun, D. (1996). The rDNA transcription machinery is assembled during mitosis in active NORs and absent in inactive NORs. *J. Cell Biol.* **133,** 235–246.

Rudloff, U. D., Eberhard, L., Tora, L., Stunnenberg, H., and Grummt, I. (1994). TBP-associated factors interact with DNA and govern species specificity of RNA polymerase I transcription. *EMBO J.* **13,** 2611–2616.

Scheer, U., Hügle, B., Hazan, R., and Rose, K. M. (1984). Drug-induced dispersal of transcribed rRNA genes and transcriptional products: Immunolocalization and silver staining of different nucleolar components in rat cells treated with 5,6-dichloro-α-D-ribofuranosylbenzimidazole. *J. Cell Biol.* **99,** 672–679.

Schnapp, G., Santori, F., Carles, C., Riva, M., and Grummt, I. (1994). The HMG box-containing nucleolar transcription factor UBF interacts with a specific subunit of RNA polymerase I. *EMBO J.* **13,** 190–199.

Shaw, P. J., and Jordan, E. G. (1995). The nucleolus. *Annu. Rev. Cell Dev. Biol.* **11,** 93–121.

Seither, P., Zatsepina, O., Hoffmann, M., and Grummt, I. (1997). Constitutive and strong association of PAF53 with RNA polymerase I. *Chromosoma* **106,** 216–255.

Seither, P., Iben, S., and Grummt, I. (1998). Mammalian RNA polymerase I exists as a holoenzyme with associated basal transcription factors. *J. Mol. Biol.* **275,** 43–53.

Sirri, V., Roussel, P., and Hernandez-Verdun, D. (1999). The mitotically phosphorylated form of the transcription termination factor TTF-1 is associated with the repressed rDNA transcription machinery. *J. Cell Sci.* **112,** 3259–3268.

Szöllösi, M., Debey, P., Szöllösi, D., Rime H., and Vautier, D. (1991). Chromatin behavior under influence of puromycin and 6-DMAP at different stages of mouse oocyte maturation. *Chromosoma* **100,** 339–354.

Takeuchi, I. K. (1984). Electron-microscopic study of silver staining nucleoli in growing oocytes of rat ovaries. *Cell Tissue Res.* **236,** 249–255.

Taylor, K. D., and Piko, L. (1982). Expression of ribosomal genes in mouse oocytes and early embryos. *Mol. Reprod. Dev.* **31,** 182–188.

Telford, N. A., Watson, A. J., and Schultz, G. A. (1990). Transition from maternal to embryonic control in early mammalian development: A comparison of several species. *Mol. Reprod. Dev.* **26,** 90–100.

Tesarik, J., Kopecny, V., and Kurilo, E. (1984). Pre-ovulatory RNA synthesis in human oocytes of large antral follicles. *Histochem. J.* **16,** 438–440.

Tuan, J. C., Zhai, W., and Comai, L. (1999). Recruitment of TATA-binding protein-TAFI complex SL1 to the human ribosomal DNA promoter is mediated by the carboxy-terminal activation domain of upstream binding factor (UBF) and is regulated by UBF phosphorylation. *Mol. Cell Biol.* **19,** 2872–2879.

Vautier, D., Besombes, D., Chassoux, D., Aubry, F., and Debey, P. (1994). Redistribution of nuclear antigens linked to cell proliferation and RNA processing in mouse oocytes and early embryos. *Mol. Reprod. Dev.* **38,** 119–130.

Verheggen, C., Panse, S. L., Almouzni, G., and Hernandez-Verdun, D. (1998). Presence of pre-rRNAs before activation of polymerase I transcription in the building process of nucleoli during early development of Xenopus laevis. *J. Cell Biol.* **142,** 1167–1180.

Verlhac, M.-H., Kubiac, J. Z., Clarke, H. J., and Maro, B. (1994). Microtubule and chromatin behavior follow MAP kinase activity but not MPF activity during meiosis in mouse oocytes. *Development* **120,** 1017–1025.

Voit, R., Hoffmann, M., and Grummt, I. (1999). Phosphorylation by G1-specific cdk–cyclin complexes activates the nucleolar transcription factor UBF. *EMBO J.* **18,** 1891–1899.

Voit, R., Schnapp, A., Kuhn, A., Rosenbauer, H., Hirschmann, P., Stunnenberg, P., and Grummt, I. (1992). The nucleolar transcription factor mUBF is phosphorylated by casein kinase II in the C-terminal hyperacidic tail which is essential for transactivation. *EMBO J.* **11,** 2211–2218.

Wassarman, P. M. (1988). The mammalian ovum. *In* "The Physiology of Reproduction" (E. Knobil and J. Neill, Eds.), pp. 69–102. Raven Press, New York.

Wassarman, P. M., and Letourneau, G. E. (1976). RNA synthesis in fully-grown mouse oocytes. *Nature* **261,** 73–74.

Weisenberger, D., and Scheer, U. (1995). A possible mechanism for the inhibition of ribosomal RNA gene transcription during mitosis. *J. Cell Biol.* **129,** 561–575.

Winking, H., Nielsen, U., and Gropp, A. (1980). Variable positions of NORs in Mus musculus. *Cytogenet. Cell Genet.* **26,** 158–164.

Winston, N. J., and Maro B. (1999) Changes in the activity of type 2A protein phosphatases during meiotic maturation and first mitotic cell cycle in mouse oocytes. *Biol. Cell* **91,** 175–183.

Zatsepina, O. V., Todorov, I. T., Philipova, R. N., Krachmarov, C. P., Trendelenburg, M. F., and Jordan, E. G. (1997). Cell cycle-dependent translocations of a major nucleolar phosphoprotein, B23, and some characteristics of its variants. *Eur. J. Cell Biol.* **73,** 58–70.

Zatsepina, O. V., Voit, R., Grummt, I., Spring, H., Semenov, M. V., and Trendelenburg, M. F. (1993). The RNA polymerase I-specific transcription initiation factor UBF is associated with transcriptionally active and inactive ribosomal genes. *Chromosoma* **102,** 599–611.

Zuccotti, M., Piccinelli, A., Rossi, P. G., Garanga, S., and Redi, C. A. (1995). Chromatin organization during mouse oocyte growth. *Mol. Reprod. Dev.* **41,** 479–485.

Zuccotti, M., Rossi, P. G., Martinez, A., Garanga, S., Forabosco, A., and Redi, C. A. (1998). Meiotic and developmental competence of mouse antral oocytes. *Biol. Reprod.* **58,** 700–704.